ELSEVIER

Interface affected zone for optimal strength and ductility in heterogeneous laminate

C.X. Huang [1,*,†], Y.F. Wang [1,†], X.L. Ma [2], S. Yin [3], H.W. Höppel [4], M. Göken [4], X.L. Wu [5,*], H.J. Gao [3,*], Y.T. Zhu [2,6,*]

[1] School of Aeronautics and Astronautics, Sichuan University, Chengdu 610065, China
[2] Department of Materials Science and Engineering, North Carolina State University, Raleigh, NC 27695, USA
[3] School of Engineering, Brown University, Providence, RI 02912, USA
[4] Department of Materials Science and Engineering, Institute I: General Materials Properties, Friedrich-Alexander University of Erlangen-Nürnberg, Martensstr. 5, 91058 Erlangen, Germany
[5] State Key Laboratory of Nonlinear Mechanics, Institute of Mechanics, Chinese Academy of Sciences, Beijing 100190, China
[6] Jiangsu Key Laboratory of Advanced Micro & Nano Materials and Technology, Nanjing University of Science and Technology, Nanjing 210094, China

Interfaces have been reported to significantly strengthen and toughen metallic materials. However, there has been a long-standing question on whether interface-affected-zone (IAZ) exists, and how it might behave. Here we report *in situ* high-resolution strain mapping near interfaces in a copper–bronze heterogeneous laminate, which revealed the existence of IAZs. Defined as the zone with strain gradient, the IAZ was found to form by the dislocations emitted from the interface. The IAZ width remained largely constant with a magnitude of a few micrometers with increasing applied strain. Interfaces produced both back stress strengthening and work hardening, which led to both higher strength and higher ductility with decreasing interface spacing until adjacent IAZs started to overlap, after which a tradeoff between strength and ductility occurred, indicating the existence of an optimum interface spacing for the best mechanical properties. These findings are expected to help with designing laminates and other heterogeneous metals and alloys for superior mechanical properties.

Introduction

The mechanical properties of materials are largely controlled by their internal interfaces, including grain boundaries, phase boundaries, twin boundaries, lamella boundaries, etc. [1,2]. By trial and error, mankind has learned to utilize interfaces to produce metals with superior strength and ductility almost two thousand years ago [2]. For example, the Beilian steel was processed by multiple forging and folding to make strong and tough swords in China in the 2nd century [2]. The Damascus steel was used to make blades from 5th century to 19th century [3,4]. A common feature of these ancient materials is their layered or lamella structures with high density of internal interfaces.

A metallic material is either strong or ductile, but rarely both at the same time [5,6]. Coarse-grained (CG) metals usually have high ductility but low strength. Refining grains to the nanocrystalline regime in the last few decades has significantly increased the strength, but this is accompanied with the sacrifice of ductility [7]. In recent years, extensive work has been reported on metals with high density of interfaces [8,9], including laminated metals with superior mechanical properties [10–15], gradient materials with high strength, extra strain hardening and good ductility [16–22], heterogeneous lamella structures with the high strength of ultrafine-grained metal and the high ductility of CG metal [1], metals with growth and deformation twins [23–25], etc. These reports suggest that internal interfaces can be designed to produce superior mechanical properties.

* Corresponding authors at: Department of Materials Science and Engineering, North Carolina State University, Raleigh, NC 27695, USA (Y.T. Zhu).
E-mail addresses: Huang, C.X. (chxhuang@scu.edu.cn), Wu, X.L. (xlwu@imech.ac.cn), Gao, H.J. (huajian_gao@brown.edu), Zhu, Y.T. (ytzhu@ncsu.edu).
† These two authors contributed equally to this work.

 https://doi.org/10.1016/j.mattod.2018.03.006

In spite of the above progresses, it remains unclear what mechanisms are activated at interfaces to affect the mechanical properties. The superior mechanical properties observed in lamella and gradient materials have been attributed to back-stress strengthening and back-stress work hardening caused by the piling up of geometrically necessary dislocations (GNDs) at internal interfaces [1,11,26]. These GNDs were generally assumed to be generated by Frank-Read sources and blocked by the interfaces. However, there are also opinions that Frank-Read sources rarely exist in metals [27]. A study on laminated structure reveals possible existence of an optimum layer thickness for the best mechanical properties [11]. Post-mortem examination after tensile testing revealed possible piling-up of GNDs near interfaces [8]. These observations suggest that interface-affected zone (IAZ) likely exists, but this also raised issues on how the IAZs form and evolve during the plastic deformation.

The strain gradient near the interfaces developed during tensile testing cannot be fully preserved post-mortem because the dislocation pile-up configuration evolves during unloading, which presents a great challenge to quantifying the effect of interface on the mechanical behavior. What makes it more challenging is the discrete nature of dislocation pile-up events, which makes it necessary to study the strain gradient statistically along interfaces, rather than local images using conventional transmission electron microscopy (TEM). In this study, we combine the *in situ* high-resolution strain mapping, mechanical testing and theoretical modeling to investigate these issues. Copper–bronze laminates were used in this study for their stable interfaces [11].

Heterogeneous copper–bronze laminates

Laminates consisting of CG copper layers and nanostructured (NS) bronze (Cu–10%wt.Zn) layers were fabricated by accumulative roll bonding (Fig. 1a). Microhardness was measured using nanoindentation as 0.95 GPa in the CG copper layer, and 2.20 GPa in the NS bronze layer in all laminates (Fig. 1b). The layer thickness was systematically varied from 125 μm to 3.7 μm by cold rolling (Fig. S1). All laminate samples were annealed before tensile testing to produce an average grain size of about 4.8 μm in the Cu layer and 100 nm in the bronze layer (Figs. 1c, d and S1). Such large differences in grain size and hardness are expected to produce a significant mechanical incompatibility across the interface during plastic deformation, which consequently generates high back stress [8].

Interface-affected-zone

In this study we developed a high-resolution digital image correlation (DIC) analysis technique to map *in situ* local strain

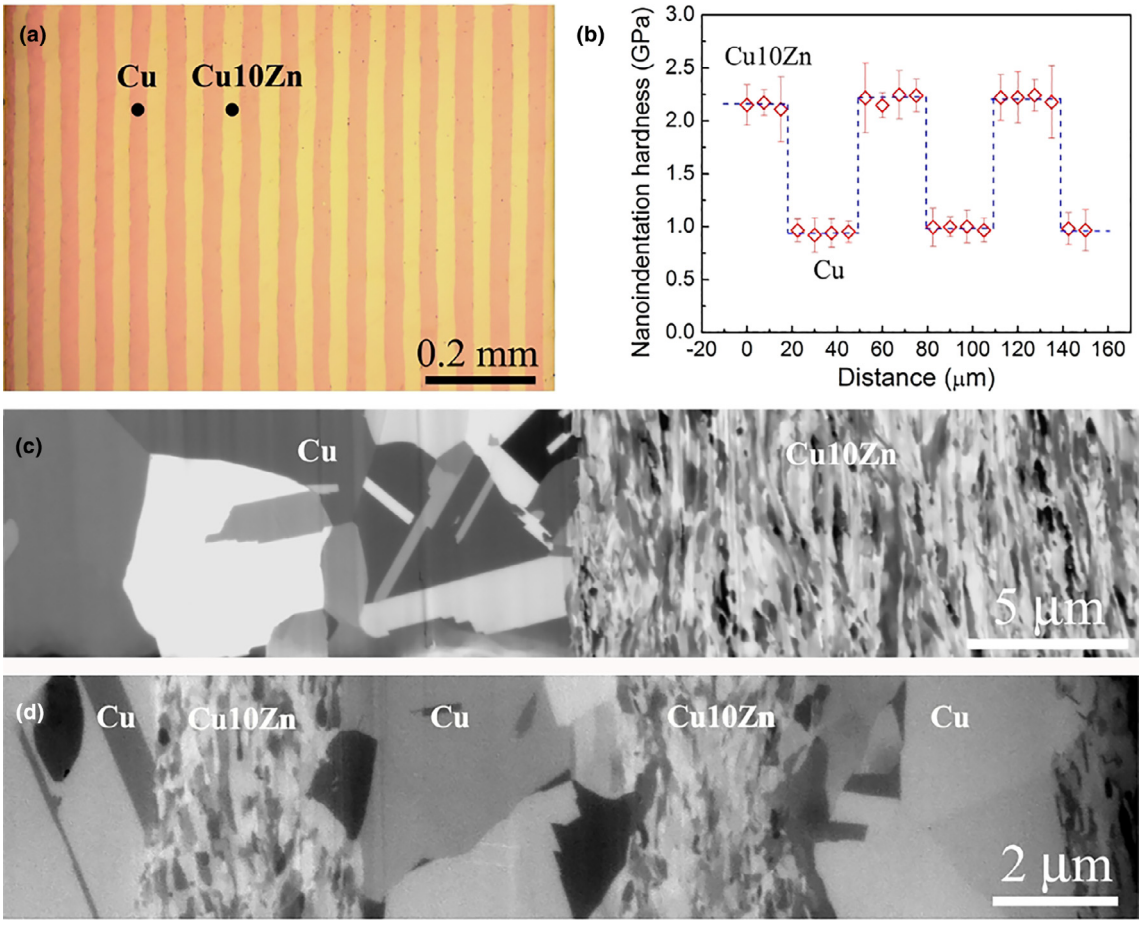

FIGURE 1

Heterogeneous copper–bronze laminates. (a) Optical image of the laminate with mean layer thickness of 31 μm. (b) Hardness profile from nanoindentation. (c) Ion channeling contrast microscopy (ICCM) image showing a typical interface in the laminate with mean layer thickness of 62 μm. (d) ICCM image showing the microstructure in a laminate with mean layer thickness of 3.7 μm.

distribution and evolution near selected interfaces during tensile testing inside a scanning electron microscope (SEM) (see the Materials and Methods section for more details). Fig. 2a, b shows the strain distributions in the tensile direction ε_{yy} and thickness direction ε_{xx} with increasing applied strain. As shown, many discrete shear bands were developed at about 45° to the loading direction in both the CG Cu and NS bronze layers. The average ε_{yy} strain at and near the interface is about the same as that away from the interface (Figs. 2c and S2). In other words, the average ε_{yy} strain is uniformly distributed along the thickness. This is because all layers in the laminate are continuous and subjected to the same applied strain in the tensile direction. However, the strain in the thickness direction, ε_{xx}, concentrates on each side of the interfaces to form an obvious zone with strain gradient, as shown in Fig. 2b, c. This zone with strain gradient is here defined as the interface-affected zone (IAZ).

Plastic strain in a metal is typically dominated by the nucleation and propagation of dislocations. The higher ε_{xx} strain at the interface indicates that dislocations are emitted from the interfaces as proposed by Li and Murr [27,28]. This is opposite to the conventional belief that dislocations are emitted from Frank-Read sources and piled up at interfaces [8,29], which will produce the lowest plastic strain at the interface.

To quantify the width of the IAZs, the ε_{xx} strain peaks across the interfaces (Figs. 2c and S2) can be fitted by a Gaussian distribution function, from which two important parameters, the width W at half maximum of the strain peak and strain peak intensity H can be extracted, as illustrated in Fig. 2d. The width at the half strain peak can be assumed equal to half of the peak width at its base. In other words, W can be considered as the IAZ width. Fig. 2e shows that the IAZ width remains largely constant with increasing applied tensile strain. *This indicates*

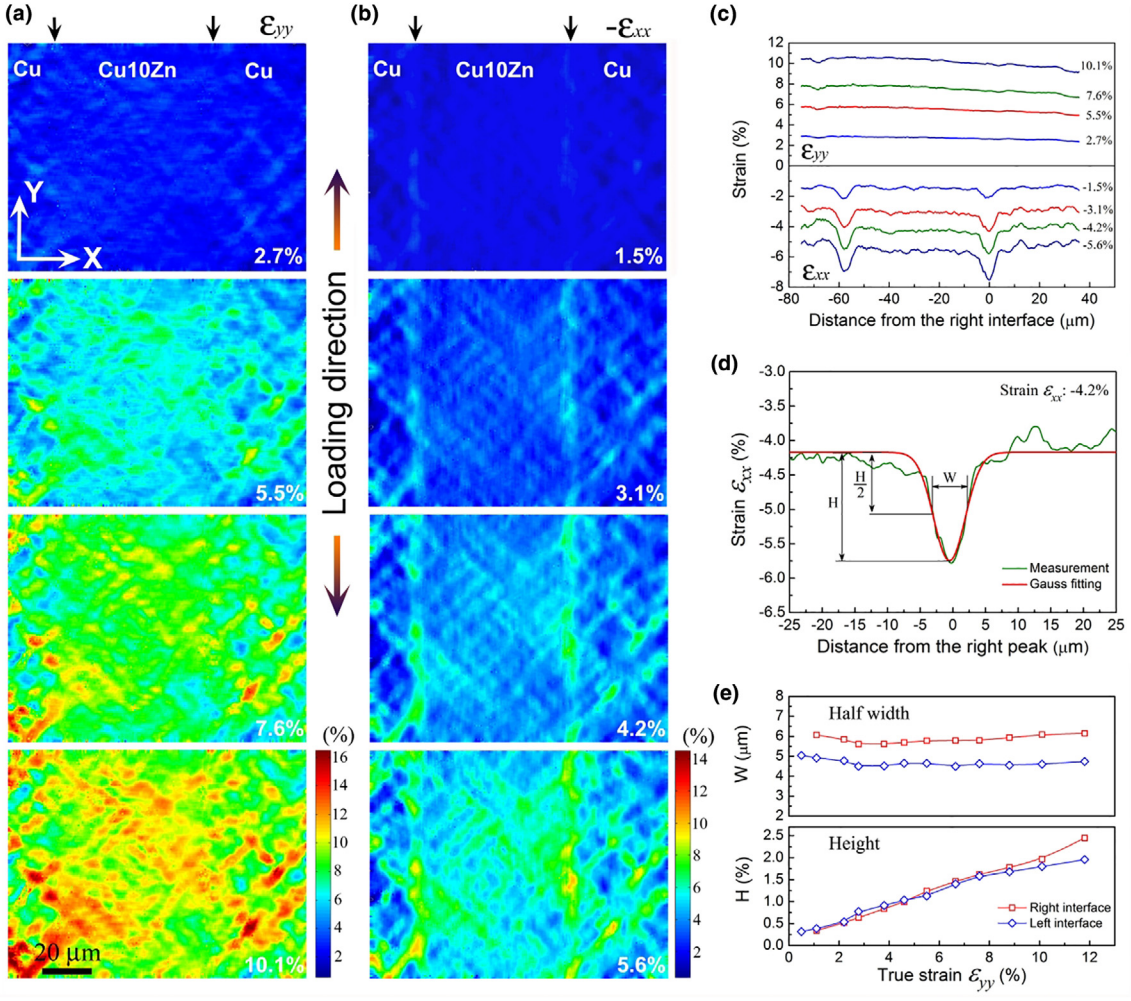

FIGURE 2

Interface-affected-zone measured by *in situ* high-resolution DIC technique in a Cu–bronze laminate. (a) The distribution of strain $\varepsilon_{yy} = du_y/dy$ with increasing applied tensile strain, where u_y is the displacement in tensile direction. (b) The distribution of strain $\varepsilon_{xx} = du_x/dx$ with increasing applied tensile strain, where Y is the tensile direction and X is the sample thickness direction. The top black arrows indicate the position of interfaces. (c) The evolution of statistical average strain, ε_{yy} and ε_{xx}, as a function of distance from the right interface. The ε_{xx} strain peaks at the two interfaces indicate a high strain gradient near them. (d) The definition and calculation of IAZ based on strain peak. Here, H denotes the intensity of strain peak and W is the width at half of the peak maximum ($H/2$), referred to as half width for simplicity. W also equals the width of the IAZ. (e) The evolution of the half width (W) and strain intensity (H) with increasing applied tensile strain. The half widths of the two ε_{xx} strain peaks near interfaces remain largely constant, while their intensities increase with increasing applied tensile strain.

the existence of a characteristic IAZ width that does not change with the applied tensile strain. However, the intensity of the plastic strain peak in the IAZ increases with increasing tensile strain (Fig. 2e), which suggests that the strain gradient becomes larger with increasing tensile strain.

Theoretical modeling of the critical interface-affected-zone width

According to the dislocation ledge source model [27,28], the ledges on the interface between the CG copper and NS bronze layers could act as sources to emit dislocations, as observed here (Fig. 2). Upon loading, the ledge sources on the interface will be activated and produce arrays of dislocations as shown in Fig. 3, which forms the IAZ.

Li and co-workers [27,28] have shown that the dislocation emission due to ledge sources gives rise to similar length scale as the classical dislocation pile up model [29] near an interface. In this model, the length of the emitted dislocation array l, corresponding to the width of the IAZ, can be expressed as

$$l = \frac{\mu n b}{\pi(1-\nu)\sigma} \tag{1}$$

where μ is the shear modulus, n the number of dislocations in the array, b the burgers vector, ν Poisson's ratio, and σ the applied stress.

The local stress field at the root of the dislocation array is:

$$\sigma_{xy} \cong \sigma\sqrt{\frac{l}{x}}, \quad \text{for } x \ll \frac{l}{2} \tag{2}$$

To estimate the critical width of the IAZ, we assume the strength of the interface to be on the order of μ and the ledge sources are located at a few Burgers vectors away from the interface. Plugging these parameters into Eq. (2) yields:

$$l_{IAZ} \approx \left(\frac{\mu}{\sigma_y}\right)^2 b \tag{3}$$

It can be estimated that the derived length scale of IAZ is on the order of a few micrometers, which is consistent with our experiment observation (Fig. 2b, e). This length scale is also consistent with the characteristic length associated with strain gradient plasticity $l_{GDN} \sim \left(\frac{\mu}{\sigma_y}\right)^2 b$ [30,31].

Mechanical behaviors controlled by interfacial spacing

Fig. 4a shows that the yield strength and flow stress increased with decreasing interface spacing, which is expected since the interfaces enhance strength and flow stress [1,17]. It is also found that the work hardening capability increased with decreasing interface spacing (Fig. 4b), which should help with retaining ductility [6,32]. Fig. 4c demonstrates that the ductility first increased with decreasing interface spacing, reaching its maximum when the interface spacing is about 15 μm, and then decreased with further reduction of the interface spacing. In other words, there exists an optimum interface spacing for the best combination of strength and ductility. It should be noted that this optimum interface spacing is about twice of the critical IAZ width. In other words, the IAZ zones from adjacent interfaces start to overlap with each other below this optimum spacing.

Fig. 4d indicates that the relationship between the interface spacing h and the flow stress σ can be described as $\sigma = \sigma_0 h^n$, where σ_0 and n are constants. The interfaces are expected to produce strong back-stress, which can be measured by unloading–reloading experiments (Figs. 4e and S3), using a recently proposed procedure [26]. Fig. 4f shows that the back-stress strengthening in the sample is much higher than the effective stress strengthening

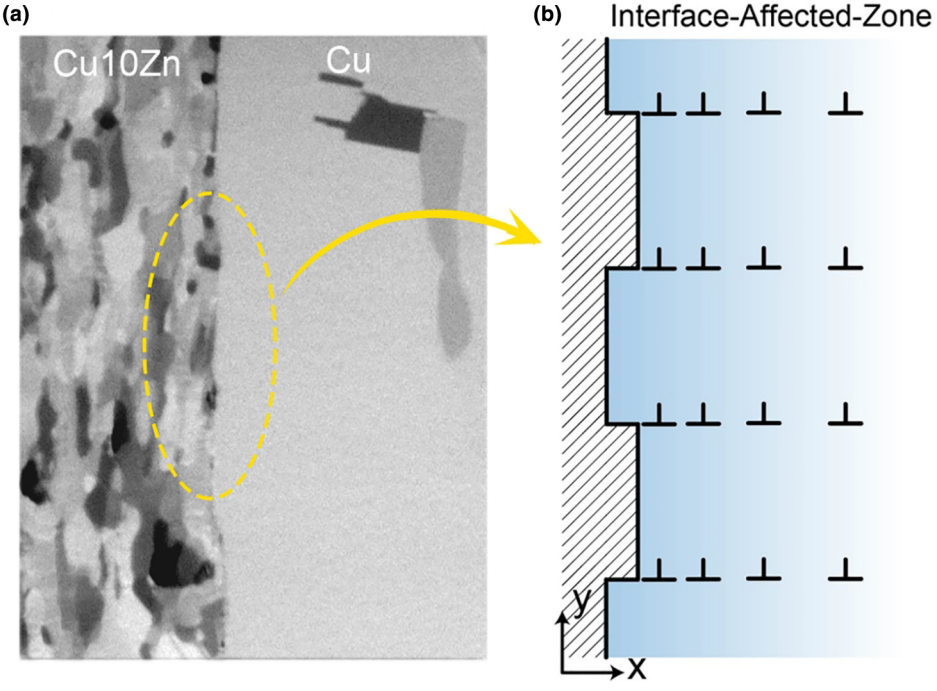

FIGURE 3

Interface-affected-zone by dislocation ledge source model. (a) ICCM micrograph of Cu–bronze interface. (b) Schematic illustrations of IAZ by dislocation source model.

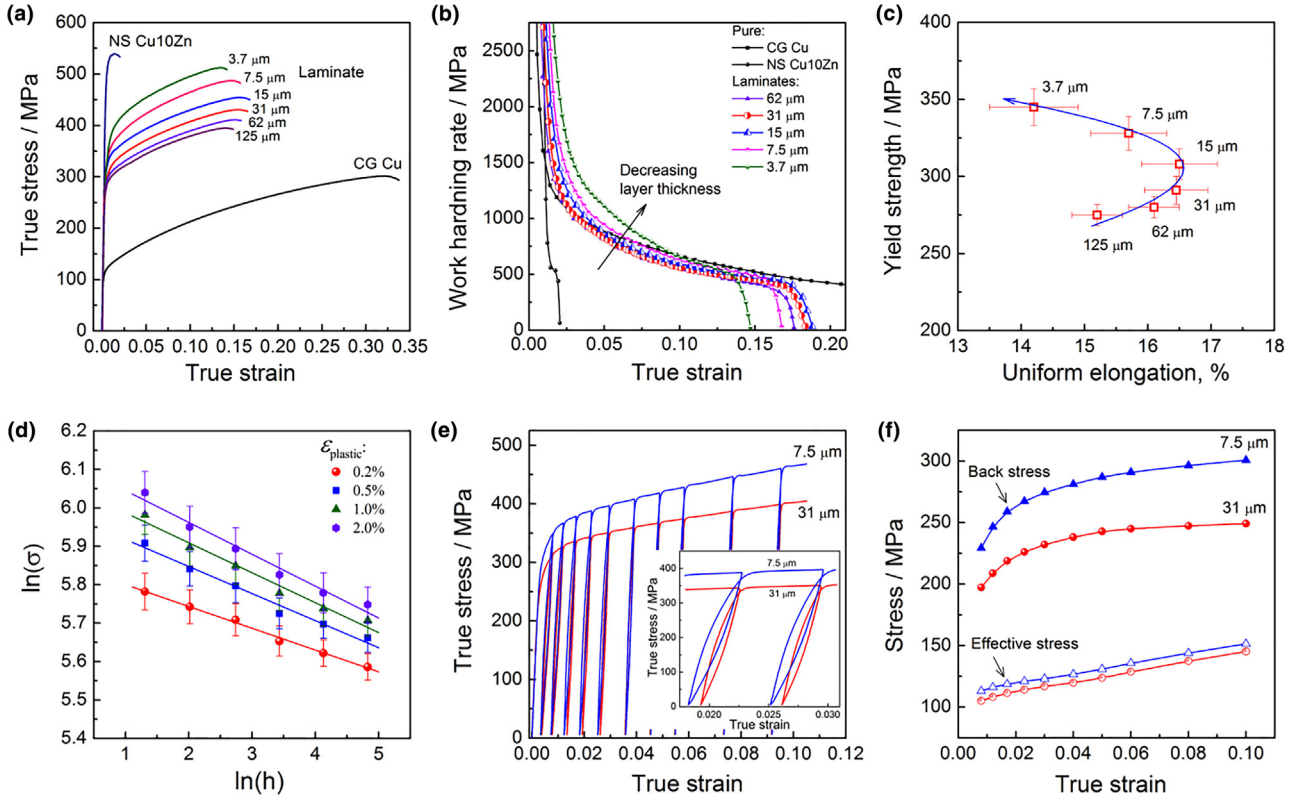

FIGURE 4

The effect of interface spacing on the mechanical behaviors of the Cu–bronze laminates. (a) True stress–strain curves vs. interface spacing. (b) Smaller interface spacing produces higher work hardening. (c) Strength–ductility relationship vs. interface spacing *h*. The given numbers reflect for the interface spacing. (d) Linear relationship between ln(*σ*) and ln(*h*). (e) Unloading–reloading curves for back stress and effective-stress measurements. (f) The effect of interface spacing on the evolution of back stress and effective stress with plastic strain.

caused by pure dislocation density strengthening. The back-stress is primarily caused by GNDs that were emitted from and piled-up near the interfaces. More GNDs are expected with higher interface density, i.e., decreasing interface spacing. It is also shown in Fig. 4f that the back-stress increased quickly at the beginning of plastic deformation (<2%) and then slowed down as plastic strain increases, suggesting that the back-stress work hardening is most effective in the early stage of plastic deformation. In contrast, the effective stress increased almost linearly with applied strain, indicating a largely constant contribution to work hardening rate. The effective stress, τ_e, is associated with dislocation density [31]: $\tau_e = \alpha\mu b\sqrt{\rho}$, where α is a constant between 0.2 and 0.5, and ρ is dislocation density. Since $d\tau_e/d \in =$ constant, as indicated in Figs. 4f and S3, it can be derived that $\sqrt{\rho} \propto \varepsilon$.

Discussion and summary

It is found that a characteristic IAZ was formed near interfaces in heterogeneous laminates. The IAZ was defined as the zone with strain gradient on one side of an interface. There is consensus that the piling up of GNDs near interface produces strain gradient [30,31,33,34]. We have found in an earlier work that GND density gradient was developed near the interface in the CG–Cu/NS–bronze sample with increasing applied strain [11], which suggests that the GND density gradient is related to the strain gradient observed here in the DIC measurement.

As shown in Fig. 2d, e, although the critical IAZ width remained largely constant with increasing tensile strain, the strain intensity in the IAZ increased, leading to higher strain gradient and back-stress work hardening. During plastic deformation, the emitted dislocations from dislocation sources at the interface form the IAZ with a characteristic length scale on the order of several micrometers, which corresponds to an inherent internal material length associated with the storage of GNDs. This is consistent with the fact that the critical width of IAZ is also the characteristic length in strain gradient plasticity [30,31]. Therefore, it can be expected that the effect of GNDs is maximized when the interface spacing become comparable to twice of the IAZ width at which the IAZs from adjacent interfaces touch each other, as shown in our experiment.

The critical width of the IAZ is about 5–6 μm, which is very close to half of the optimum interface spacing for the highest ductility of laminate (Fig. 4a, c). This suggests that when the IAZs from adjacent interfaces approach each other with decreasing interface spacing, their IAZs may start to overlap, which limits the effectiveness of back-stress hardening, and consequently leads to weaker ability to retain ductility.

According to the experimental observation [27], when the interface ledge sources were activated, the average number of dislocations in each emission profile becomes saturated around 1% of plastic strain. This is also consistent with our observation that the width of the critical IAZ does not change with the applied tensile strain (Fig. 2e).

Fig. 5 compares the strength and ductility of the Cu–bronze laminate with those of conventional homogeneous Cu and bronze [35–41], which further demonstrates that the laminate spacing can be optimized to produce superior combinations of strength and ductility that are not accessible to their homogeneous counterparts. The optimum/critical interface spacing revealed in Figs. 4c and 5 has significant implications in the design of the heterogeneous structures [8,9] for superior mechanical properties. The key principle is to maximize the back-stress strengthening and back-stress work hardening. When the interface spacing is too large, not enough back-stress is produced. However, when the interface spacing is too small, the IAZs overlap with each other, leaving insufficient space for dislocation to pile-up, which then limits the work hardening capability for retaining ductility. Therefore, heterogeneous structures should be designed with an optimum interfacial spacing comparable to twice of the IAZ width.

Materials and methods

Material preparation

Cu–bronze laminates were processed by accumulative rolling bonding (ARB) using commercial Cu (99.9%) and bronze (Cu–10 wt.%Zn) sheets [11]. The layer thickness was systematically varied from 125 μm to 3.7 μm by cold rolling. All laminate samples were annealed at 220 °C for 2 h so that recrystallization occurs in Cu layers but not in bronze layers (Fig. S1).

Microstructural observations

The laminate microstructure was characterized by optical microscopy, ion channeling contrast microscopy (ICCM) in scanning electron microscope (SEM) and transmission electron microscopy (TEM). ICCM was performed under an FEI Quanta 3D FEG dual-beam instrument, and TEM was conducted in a JEM-2010F microscope. Sample preparation for microstructural observations can be found in our previous works [10,11].

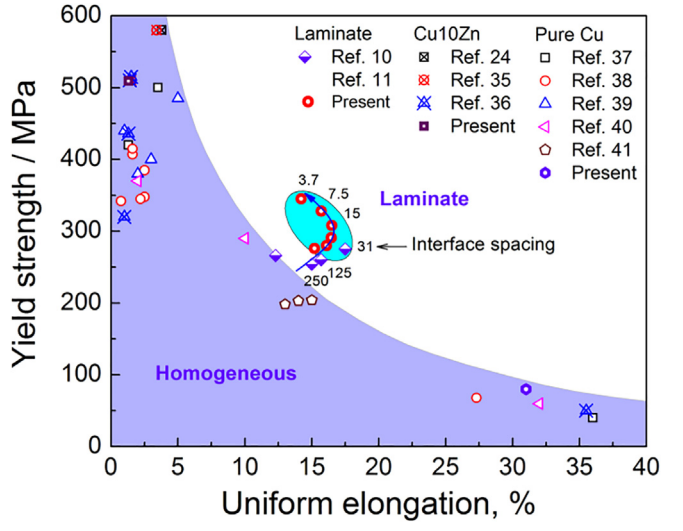

FIGURE 5

Comparison of strength and ductility (uniform elongation) between the laminated CG–Cu/NS–bronze samples and the conventional homogenous materials. An optimum layer thickness exists for the best combination of strength and ductility. (See above-mentioned references for further information.)

DIC characterization

An *in situ* quasi-static micro-tensile stage was made in house and set up in a JSM-6510LV microscope. Taking reference images from 10 equidistant points in the lateral surface of the gauge section (see the coordinate system in Fig. S4), a 0.2% engineering strain was applied for the first loading and then a large strain increment of 1.1% was applied until sample failure. Digital images were taken after each strain increment. 2D DIC calculations were performed with a subset size of 25 × 25 pixel^2, and a step spacing of 3 pixel, as shown in Fig. S5.

Before performing DIC imaging, random pattern with appropriate scale and resolution is needed to cover the sample surface as strain markers. In this work, electrochemical etching was used as an effective patterning method [42], using a solution comprising 10 g $FeCl_3$, 100 ml H_2O, and 2.5 ml HCl dilute solution, under a DC voltage of 0.7 V for 15 s. Samples before and after etching were tested in tension and the resulting stress–strain curves were identical, indicating that the etching had negligible effect on the measured mechanical behavior. Fig. S5 shows the typical digital speckle image taken under SEM, covering 715 × 550 pixel^2 effective area with a spatial resolution of 171 nm/pixel. The mean intensity gradient is equal to 51.2, which is of high quality for the speckle patterns used in DIC [43].

Mechanical testing

Uniaxial tensile and loading–unloading–reloading tests were performed using dog-bone shaped tensile samples with a gauge length of 12 mm and a width of 2 mm at a strain rate of 5×10^{-4} s^{-1}. An extensometer was used to calibrate strain during uniform elongation and each test was repeated for at least 3 times. Nanoindentation experiments were conducted using an MTS Nanoindenter XP equipped with a Berkovich pyramid indenter. Neighboring indents were separated by distances larger than 10 μm to avoid the influence of the plastic zone around the indent and each datum given in the text was averaged from 5 indentations.

Acknowledgments

Financial support from the National Key R&D Program of China (2017YFA0204402 and 2017YFA0204403) and National Natural Science Foundation of China (11672195 and 11572328) are acknowledged. C.X.H. is funded by Sichuan Youth Science and Technology Foundation (2016JQ0047). Y.T.Z. is funded by the US Army Research Office. H.J.G is funded by National Science Foundation through Grant DMR-1709318. H.W.H and M.G. gratefully acknowledge the funding of the German Research Council (DFG) which, within the framework of its 'Excellence Initiative' supports the Cluster of Excellence 'Engineering of Advanced Materials' at the University of Erlangen-Nürnberg.

Author contributions

C.X.H. and Y.F.W. developed the high-resolution DIC technique and designed experiments. C.X.H., Y.F.W., X.L.M., X.L.W., and Y.T.Z. conceived the initial research issues. C.X.H., Y.F.W.

X.L.W., and Y.T.Z. analyzed the data. S.Y. and H.J.G. performed the theoretical analysis. H.W.H. and M.G. processed the laminated sample using ARB. All contributed to discussions. C.X.H., Y.F.W., X.L.W. H.J.G., and Y.T.Z. wrote the paper.

Appendix A. Supplementary data

Supplementary data associated with this article can be found, in the online version, at https://doi.org/10.1016/j.mattod.2018.03.006.

References

[1] X.L. Wu et al., Proc. Natl. Acad. Sci. U.S.A. 112 (2015) 14501–14505.
[2] J.T. Wang, Mater. Sci. Forum 503–504 (2006) 363–370.
[3] J.D. Verhoeven, A.H. Pendray, W.E. Dauksch, JOM 50 (1998) 58–64.
[4] J. Wadsworth, O.D. Sherby, Prog. Mater. Sci. 25 (1980) 35–68.
[5] R.Z. Valiev et al., J. Mater. Res. 17 (2002) 5–8.
[6] Y.T. Zhu, X.Z. Liao, Nat. Mater. 3 (2004) 351–352.
[7] R.Z. Valiev et al., Mater. Res. Lett. 4 (2016) 1–21.
[8] X.L. Wu, Y.T. Zhu, Mater. Res. Lett. 5 (2017) 527–532.
[9] E. Ma, T. Zhu, Mater. Today 20 (2017) 323–331.
[10] X.L. Ma et al., Scr. Mater. 103 (2015) 57–60.
[11] X.L. Ma et al., Acta Mater. 116 (2016) 43–52.
[12] A. Misra, J.P. Hirth, R.G. Hoagland, Acta Mater. 53 (2005) 4817–4824.
[13] I.N. Mastorakos et al., J. Mater. Res. 26 (2011) 1179–1187.
[14] M.M. Wang et al., Acta Mater. 85 (2015) 216–228.
[15] J.S. Carpenter et al., Mater. Res. Lett. 3 (2015) 50–57.
[16] K. Lu, Science 345 (2014) 1455–1456.
[17] X.L. Wu et al., Proc. Natl. Acad. Sci. U.S.A. 111 (2014) 7197–7201.
[18] X.L. Wu et al., Mater. Res. Lett. 2 (2014) 185–191.
[19] T.H. Fang et al., Science 331 (2011) 1587–1590.
[20] A.Y. Chen et al., Mater. Sci. Eng. A 667 (2016) 179–188.
[21] Y.J. Wei et al., Nat. Commun. 5 (2014) 3580.
[22] X.L. Wu et al., Acta Mater. 112 (2016) 337–346.
[23] K. Lu, L. Lu, S. Suresh, Science 324 (2009) 349–352.
[24] Y.H. Zhao et al., Appl. Phys. Lett. 89 (2006) 121906.
[25] C.X. Huang et al., Mater. Res. Lett. 3 (2015) 88–94.
[26] M.X. Yang et al., Mater. Res. Lett. 4 (2016) 145–151.
[27] L.E. Murr, Metall. Mater. Trans. A 47 (2016) 5811–5826.
[28] J.C.M. Li, Trans. Metall. Soc. AIME 227 (1963) 239–247.
[29] J.P. Hirth, J. Lothe, Theory of Dislocations, 2nd ed., John Wiley Sons, 1982.
[30] W.D. Nix, H. Gao, J. Mech. Phys. Solids 46 (1998) 411–425.
[31] H. Gao et al., J. Mech. Phys. Solids 47 (1999) 1239–1263.
[32] Y.T. Zhu, X.Z. Liao, X.L. Wu, Prog. Mater. Sci. 57 (2012) 1–62.
[33] M.F. Ashby, Philos. Mag. 21 (1970) 399–424.
[34] H. Gao, Y.G. Huang, Scr. Mater. 48 (2003) 113–118.
[35] X.Y. San et al., Mater. Des. 35 (2012) 480–483.
[36] P. Zhang et al., Mater. Sci. Eng. A 594 (2014) 309–320.
[37] Y.H. Zhao et al., Adv. Mater. 18 (2006) 2949–2953.
[38] F. Dalla Torre et al., Acta Mater. 52 (2004) 4819–4832.
[39] Y. Zhang, N.R. Tao, K. Lu, Acta Mater. 56 (2008) 2429–2440.
[40] P. Xue, B.L. Xiao, Z.Y. Ma, Mater. Sci. Eng. A 532 (2012) 106–110.
[41] Sh. Ranjbar Bahadori, K. Dehghani, F. Bakhshandeh, Mater. Sci. Eng. A 583 (2013) 36–42.
[42] J.C. Stinville, Acta Mater. 98 (2015) 29–42.
[43] B. Pan, Z.X. Lu, H.M. Xie, Lasers Eng. 48 (2010) 469–477.